UDK 620.175:67.017:539.38:669.295
Original scientific article/Izvirni znanstveni članek

ISSN 1580-2949
MTAEC9, 55(4)559(2021)

HOT-DEFORMATION BEHAVIOR OF HOT ISOSTATIC PRESSED Ti-6Al-4V ALLOY DURING HOT COMPRESSION

OBNAŠANJE ZLITINE Ti-6Al-4V MED VROČO DEFORMACIJO, IZVEDENO S POSTOPKOM VROČEGA IZOSTATSKEGA STISKANJA

Haijun Liu, Zhimin Zhang, Kaihua Xu, Jishi Zhang, Yong Xue*, Qiang Wang

School of Material Science and Engineering, North University of China, No. 3 Xueyuan Rd., Taiyuan 030051, China

Prejem rokopisa – received: 2020-09-15; sprejem za objavo – accepted for publication: 2021-04-29

doi:10.17222/mit.2020.180

A single-pass and multi-pass compression experiments with a Ti-6Al-4V alloy fabricated with hot isostatic pressing (HIP) were carried out on a Gleeble-1500D simulator. The true stress-strain curve, microstructure and microhardness of the alloy deformed at a total strain of about 70 % were studied. The results show that the stress value increased as the strain rate increased during each deformation pass and the same was true for the single pass. At the initial deformation stage, the flow stress increased rapidly with the increase in the strain until it reached the peak; then it showed a different softening extent, which was more obvious for the three-pass deformation than for one-pass and two-pass deformation. During the multi-pass deformation, the lamellar α phase was mainly distorted, but during the one-pass and two-pass deformation, it was bent; the spheroidisation of the lamellar α phase mainly occurred during the three-pass deformation, significantly increasing the extent of softening. Meanwhile, the degree of the spheroidized α phase and the volume fraction of β-transformed phase (β_t) increased as the strain rates increased. Finally, a tri-modal microstructure, including the β-transformed phase (β_t), lamellar α phase and equiaxed α phase was obtained during three-pass deformation. In the process of multi-pass deformation, the microhardness increased with the increase in deformation passes. When the strain rate was 1 s^{-1}, the microhardness increased from 299.5 HV and 309.1 HV to 342.6 HV with the increase in deformation passes. It was also found that the microhardness increased with an increase in the strain rate under a certain amount of deformation.

Key words: Ti-6Al-4V alloy, multi-pass deformation, flow stress, microhardness, microstructure

Avtorji v pričujočem članku opisujejo enostopenjski in večstopenjske preizkuse tlačne deformacije zlitine Ti-6Al-4V s postopkom vročega izostatskega stiskanja (HIP; angl.: Hot Isostatic Pressing) na simulatorju Gleeble-1500D. Analizirali so krivulje tečenja, mikrostrukturo in mikrotrdoto deformiranih zlitin pri približno 70 % celotni deformaciji. Rezultati preizkusov so pokazali, da stopnja deformacije narašča z vsakim prehodom (korakom) oz. povečanjem hitrosti deformacije in je enaka kot pri enostopenjski deformaciji oz. ekvivalentni deformaciji z enim prehodom z največjo hitrostjo deformacije. V začetnem stadiju deformacije nagib krivulj tečenja hitro narašča z naraščajočo hitrostjo deformacije dokler ni dosežen nek maksimum in nato pride do različne stopnje mehčanja zlitine. Pri deformaciji s tremi koraki je to bolj izrazito kot pri deformaciji v enem ali dveh korakih. Med večstopenjsko deformacijo je v glavnem prišlo do preureditve lamelarne α faze in krivljenja pri deformaciji v enem ali dveh korakih. Do sferoidizacije lamelarne α faze pa je v veliki meri prišlo pri tristopenjski deformaciji, pri kateri se je pomembno povečalo mehčanje zlitine. Medtem sta stopnja sferoidizacije in volumski delež iz β v β_t transformirano fazo naraščala z naraščajočo stopnjo deformacije. Navsezadnje avtorji ugotavljajo nastanek tri-modalne mikrostrukture pri tristopenjski deformaciji. Ta vključuje β_t transformirano fazo, lamelarno α fazo in enakoosno α fazo. Pri večstopenjski deformaciji je mikrotrdota postopoma naraščala z vsako stopnjo spremembe hitrosti deformacije. Pri hitrosti deformacije 1 s^{-1} je mikrotrdota z vsakim korakom povečanja hitrosti deformacije narasla z 299,5 HV na 309,1 HV do 342,6 HV. Prav tako avtorji ugotavljajo, da je mikrotrdota naraščala tudi s povečanjem hitrosti deformacije pri dani stopnji deformacije.

Ključne besede: zlitina Ti-6Al-4V, večstopenjska deformacija, meja tečenja, mikrotrdota, mikrostruktura

1 INTRODUCTION

Ti-6Al-4V alloy is increasingly becoming a significant material in the fields of aircraft manufacturing, national defense and automobiles due to its high strength, high rigidity, low density, good corrosion resistance, reasonable ductility and high-temperature performance.[1–4] The development of modern science and technology has higher requirements for material processing and performance, such as integral forming, rapid prototyping and high-strength forming. Therefore, different processes have been carried out on titanium alloys to optimize the mechanical properties and forming properties.[5–7] However, traditional casting and forging techniques included in integral forming usually present a series of issues such as bulk microstructure, shrinkage cavity defects and composition segregation as these result in low ductility and poor stability. Although the mechanical properties of a forged titanium alloy are better than that of a casting, the forging technology is more about getting simple structures. As we all know, the control of the α phase is one of the keys to improve the performance of Ti-6Al-4V alloy. Generally, the microstructure of a Ti-6Al-4V alloy includes a widmanstatten structure, bimodal structure and equiaxed structure.[8]

*Corresponding author's e-mail:
yongxue395@163.com (Yong Xue)

Research shows that a tri-modal structure (equiaxed α phase + secondary α phase + β transformation) can be obtained by controlling the multi-pass deformation parameters (deformation passes, deformation amount, temperature) and heat-treatment parameters.[9] Its room-temperature strength is higher than that of the equiaxed structure; the plasticity and thermal stability of the equiaxed structure are at the same level; the high-temperature performance is higher than that of the bimodal structure; and the fracture performance and fatigue performance are higher than those of the bimodal structure. Therefore, it is very important that the hot isostatic pressing (HIP) of the billet in this study is used to explore the evolution of the microstructure through the subsequent multi-pass deformation. Zhang et al.[10] studied the effect of different initial microstructures on the microstructure and flow behavior of a titanium alloy during subtransus hot deformation. Youngmoo Kim et al.[11] studied the effects of three different powder types and pressing methods on the microstructure and mechanical properties of a hot isostatic pressed Ti-6Al-4V alloy. But, there are few systematic studies of the relationship between the microstructure and properties of a HIPed Ti-6Al-4V alloy during multi-pass deformation.

In this study, single-pass and multi-pass deformations were conducted to investigate the relationship between the deformation history, flow behavior, microstructure and properties of a HIPed Ti-6Al-4V alloy. The effects of different processes and deformation conditions on the flow stress were discussed. Also, the effects of different deformation conditions on the microstructure and microhardness were studied.

2 EXPERIMENTAL PART

The hot-compressed material used in this experiment was a hot isostatic pressed (HIPed) Ti-6Al-4V alloy and its chemical composition is shown in **Table 1**. Experimental samples were obtained with hot isostatic pressing at a temperature of 920 °C and a pressure of 120 MPa applied for 2 h, and then furnace-cooled to room temperature. **Figure 1** shows the morphologies of the tested powders and the initial microstructure of the HIPed Ti-6Al-4V alloy. The initial microstructure includes parallel/staggered lamellar α phases (shown in the white pane) and a small amount of equiaxed structure (shown in the white circle) with a widmanstatten structure. The dimensions of the hot-compressed samples were ϕ8 mm × 12 mm and hot compression was carried out on the Gleeble-1500D thermo-simulation machine at different deformation parameters. **Table 2** shows the multi-pass-compression test programme. The tested samples were deformed at 950 °C and 2.4 mm for a 20-% reduction during one-pass deformation; then they were deformed at 900 °C and 2.4 mm for another 20-% reduction during two-pass deformation, and finally they were deformed at 850 °C and 3.6 mm for a 30-% reduction in three-pass deformation. All the specimens of hot compression were deformed to a maximum deformation of about 70 %. For comparison, single-pass deformation was carried out at a deformation temperature and strain rate range from (850, 900, 950) °C and 0.01 s^{-1} to 1 s^{-1}, respectively. After the deformation of each sample, the test sample was quenched immediately with water in order to keep the deformation microstructure. The tested samples were cut along the longitudinal center, polished and eroded with the Kroll corrosive agent ($HF:HNO_3:H_2O$ = 1:3:7) for 15–20 s. The microstructure of a tested simple was analyzed with an optical microscope (OM) and SU5000 scanning electron microscope (SEM).

Table 1: Chemical composition of Ti-6Al-4V alloy powder (*w*/%)

Al	V	Fe	C	N	H	O	Ti
5.87	3.94	0.36	0.67	1.22	0.012	0.09	Bal.

Table 2: The multi-pass compression test programme

One-pass def.			Two-pass def.			Three-pass def.		
T/°C	ε/%	/s^{-1}	*T*/°C	ε/%	/s^{-1}	*T*/°C	ε/%	/s^{-1}
950	20	0.01	900	20	0.01	850	30	0.01
		0.1			0.1			0.1
		1			1			1

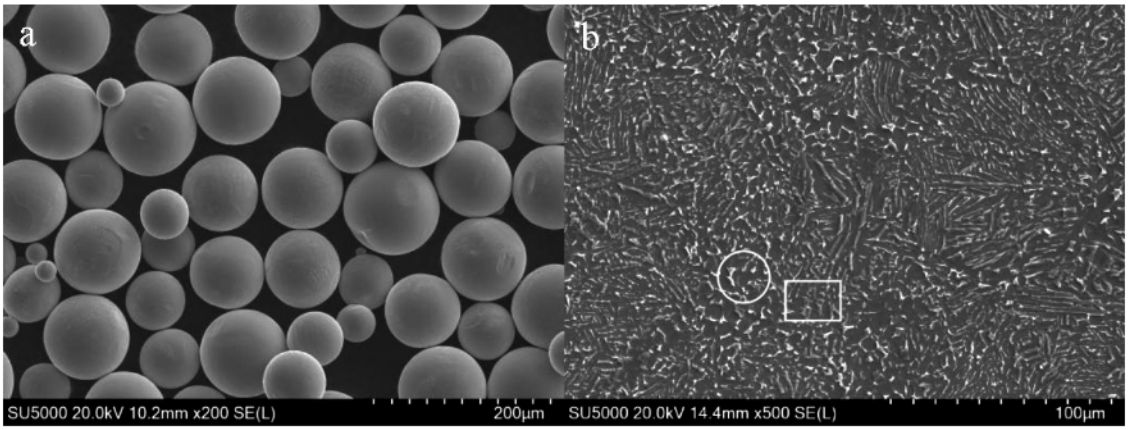

Figure 1: SEM images of the morphologies of: a) powder, b) HIPed Ti-6Al-4V alloy

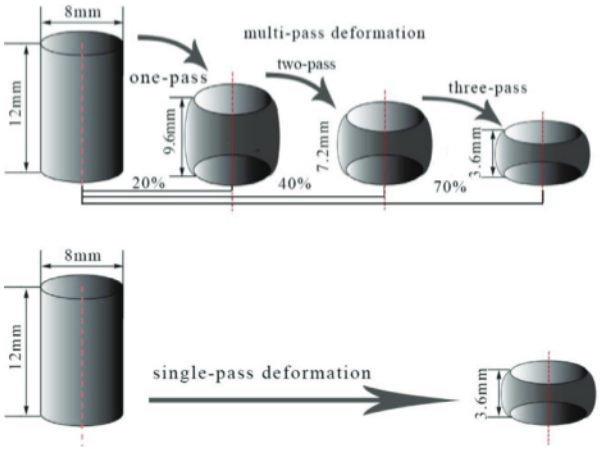

Figure 2: Schematic illustration of a multi-pass and single-pass deformed sample

3 RESULTS AND DISCUSSION

3.1. Flow-stress behaviors during hot deformation

Figures 3a and **3b** show the flow stress curves of the HIPed Ti-6Al-4V alloy after the single-pass and multi-pass deformation at the temperatures of (950, 900, 850) °C and different strain rates, respectively. **Figure 3b** shows that the flow stress increases significantly as the deformation temperature decreases and strain rate increases during the multi-pass deformation, indicating that the stress is sensitive to the deformation conditions, i.e., the temperature and strain rate. It can also be observed from **Figure 3** that, due to the effect of work hardening, the stress value suddenly increases to a peak during the initial stage of deformation, which is mainly caused by an increase in dislocations. With the increase in the strain, the stress value gradually becomes stable after the flow stress reaches the peak value, which is attributed to the balance between work hardening and softening caused by dynamic recovery and recrystallization.[12]

It can also be found that the softening degree increases with the decrease in the strain rate during single-pass deformation, but this phenomenon was not obvious during multi-pass deformation. This is mainly because the softening degree increased during multi-pass deformation. By comparing **Figures 3a** and **3b**, it can be found that the change in the stress value is very small for the peak value during one-pass deformation compared with the single-pass at 950 °C, which is mainly attributed to the same initial deformation conditions. During two-pass deformation, the peak stress is lower than that of the single-pass at the temperature of 900 °C, which is mainly attributed to the extensive flow softening and the change in the microstructure in one-pass deformation. Research shows that the flow softening is strongly related to different microstructures or localized flows, as observed in the Ti-6Al-4V alloy with a lamellar microsturcture.[13] During three-pass deformation, the influence of the softening extent on the stress is obvious with an increase in the strain rate and it is also greater than those of one-pass and two-pass deformation. This means that the dynamic softening and spheroidisation of the lamellar α phase occur due to the accumulation of deformation-activation energy during dynamic recrystallization, recovery and spheroidisation of the lamellar α phase, which counteracts the initial work hardening.[14] It can also be found from **Figure 3** that when the strain rates are higher than 0.01 s^{-1}, the peak stress during three-pass deformation is lower than during the single-pass at the deformation temperature of 850 °C, which is mainly attributed to the strain accumulation, microstructure change and a large number of nucleation sites, causing a greater softening extent compared to single-pass defomation.[15]

3.2. Microstructure investigations

3.2.1. Microstructure of the HIPed Ti-6Al-4V alloy after single-pass deformation

Figure 4 shows the OM morphologies of the HIPed Ti-6Al-4V alloy after single-pass deformation at the

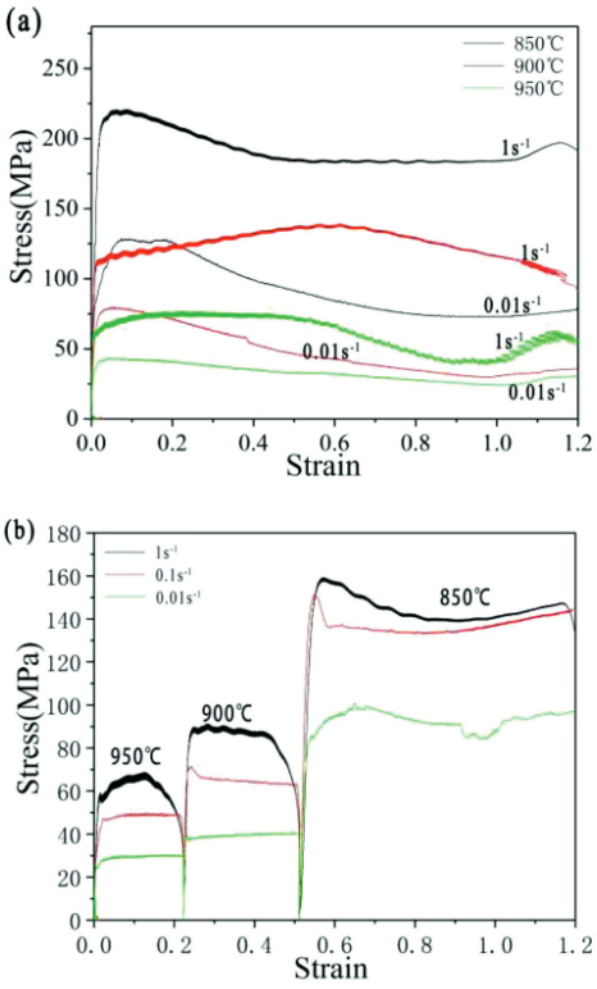

Figure 3: True stress-strain curves of HIPed TC4 alloy: a) single-pass, b) multi-pass deformation

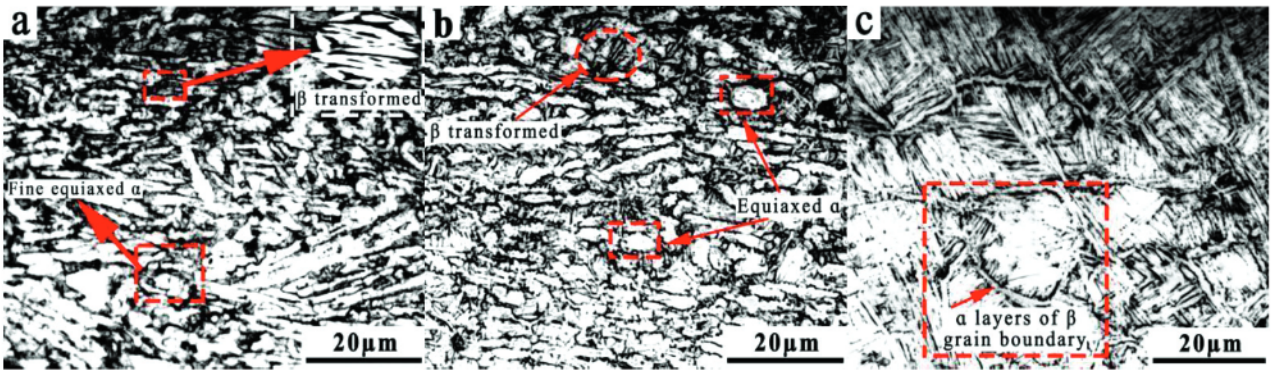

Figure 4: OM images of HIPed Ti-6Al-4V alloy after single-pass deformation at a strain rate of 1 s^{-1} and different temperatures: a) 850 °C, b) 900 °C, c) 950 °C

strain rate of 1 s^{-1} and different temperatures. When the deformation temperature was 850 °C, which was in the $\alpha + \beta$ two-phase range, the quenched microstructure of the deformed specimen was composed of equiaxed α and transformed β structure (β_t) (**Figure 4a**). According to **Table 3**, the content and average size of the equiaxed α phase were 42.2 % and 3.76 μm at the temperature of 850 °C, respectively, and then they decreased as the temperature increased. The lamellar α phase was distorted due to deformation, and a small amount of fine equiaxed α grains appeared at the same time, indicating that some dynamic recrystallization occurred at this temperature. With the increase in the deformation temperature from 850 °C to 900 °C, the volume fraction of dynamic recrystallization increased and dynamic recrystallization became more sufficient (**Figure 4b**). It can also be found from **Table 3** that the width of lamellar α decreased with the increase in the temperature, and the volume fraction of transformed β_t increased instead. This confirms the assumption that the content of the lamellar α and β transformation phase, deformed at 900 °C was larger than at the deformation temperature of 850 °C.[16] The main reason for this is that the deformation at a higher temperature provides higher energy needed for the occurrence of dynamic recovery and recrystallization (dynamic recovery is mainly used in this experiment); the obtained microstructure was also more uniform.

Table 3: Microstructure parameters of HIPed Ti-6Al-4V alloy after single-pass deformation

Temperature (°C)	Volume fraction of equiaxed α phase (%)	Size of equiaxed α (μm)	Width of lamellar α (μm)	Volume fraction of transformed β_t (%)
850	42.2	3.76	1.21	37.1
900	32.3	2.49	0.77	55.6

When the deformation temperature reached 950 °C, which was close to the β phase transition temperature, the lamellar α was sharply reduced and most of the α phase was transformed into the β phase (**Figure 4c**). It can be seen from **Figure 4c** that the β grains after deformation were coarser with an average size of 150 μm, and the grain boundaries were clear and easy to distinguish. At the same time, short lamellar α phases with different orientations precipitated in some parts of the β phase, and the distribution was not uniform. It can be found that when the deformation temperature was up to 950 °C, the transformation from α to β was easy to occur and the coarse β phase and lath martensite were obtained by water cooling after deformation. When the temperature was lower than 900 °C, the deformation was in the $\alpha + \beta$ two-phase range, and both the α and β phases were deformed. However, as the original structure was very small, the microstructure evolution in the two-phase region mainly included dynamic recrystallization and spheroidisation of the lamellar structure, which could be verified with the flow softening of the HIPed Ti-6Al-4V alloy deformed in the $\alpha + \beta$ phase field.[17]

3.2.2. Microstructure of the HIPed Ti-6Al-4V alloy after one-pass deformation

Figure 5 shows the microstructure of the HIPed Ti-6Al-4V alloy after one-pass deformation at 950 °C with different strain rates. It can be clearly seen that the microstructure of the tested specimens after one-pass deformation consists of needle-like or acicular α with an average thickness of 5 μm and β_t. Moreover, the thickness of the α layers at the β grain boundaries increased from 1.4 μm and 1.8 μm to 2.9 μm and the size of the β grains also increased as the strain rate decreased, which was mainly because the β grains had enough time to grow as the strain rate decreased.[18] Compared with the undeformed specimens, the microstructure of a compressed sample lost the original flake shape and equiaxed α phase, while only a part of the β grains were destroyed and most of them still kept the original polygonal shape. It can also be seen that a few new equiaxed β grains appeared due to dynamic recrystallization, as observed in **Figures 5a**, **5c** and **5e**.

During one-pass deformation, the primary β grains were elongated along the flow direction and some β grains began to blend, while boundary α began to fracture and was stretched simultaneously along the vertical extrusion direction; in addition, distorted and straight lamellar α appeared, as can be observed in **Figure 5**. A

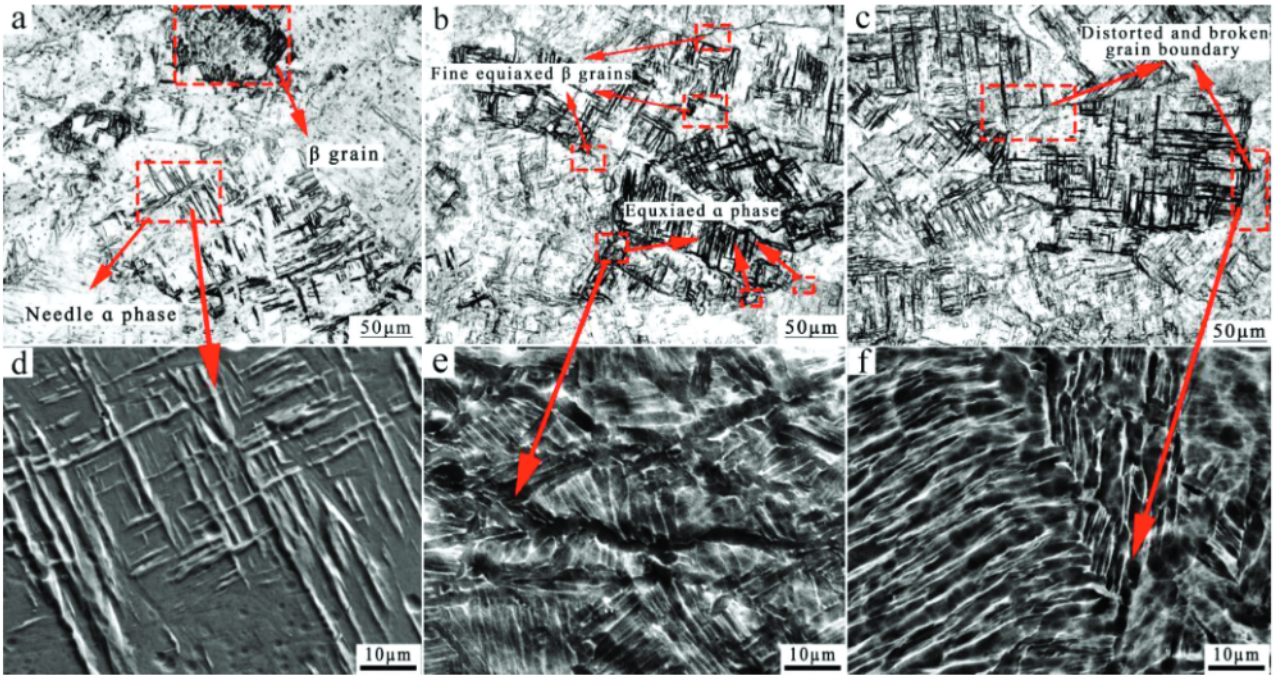

Figure 5: OM and SEM images of HIPed Ti-6Al-4V alloy after one-pass deformation at a temperature of 950 °C and different strain rates: a) and d) 1 s^{-1}, b) and e) 0.1 s^{-1}, c) and f) 0.01 s^{-1}

comparison between **Figure 1b** and **Figures 5b, 5d, 5f** shows that the size of the lamellar and needle-like α phase decreased with deformation and a finer microstructure appeared. With the increase in the strain rate, there was little difference in the microstructure (**Figure 5**). The β grains still had the shape of large polygons surrounded by a grain-boundary α layer and crisscross short α phases, while the β grain size was obviously reduced, which means that an increase in the deformation rate can refine the grains. There were a few fine equiaxed β grains at the intersection and boundary of deformed grains, and it can be seen from **Figure 5b** that the production of these equiaxed α grains was mainly concentrated at the distorted- and broken-grain boundaries. The

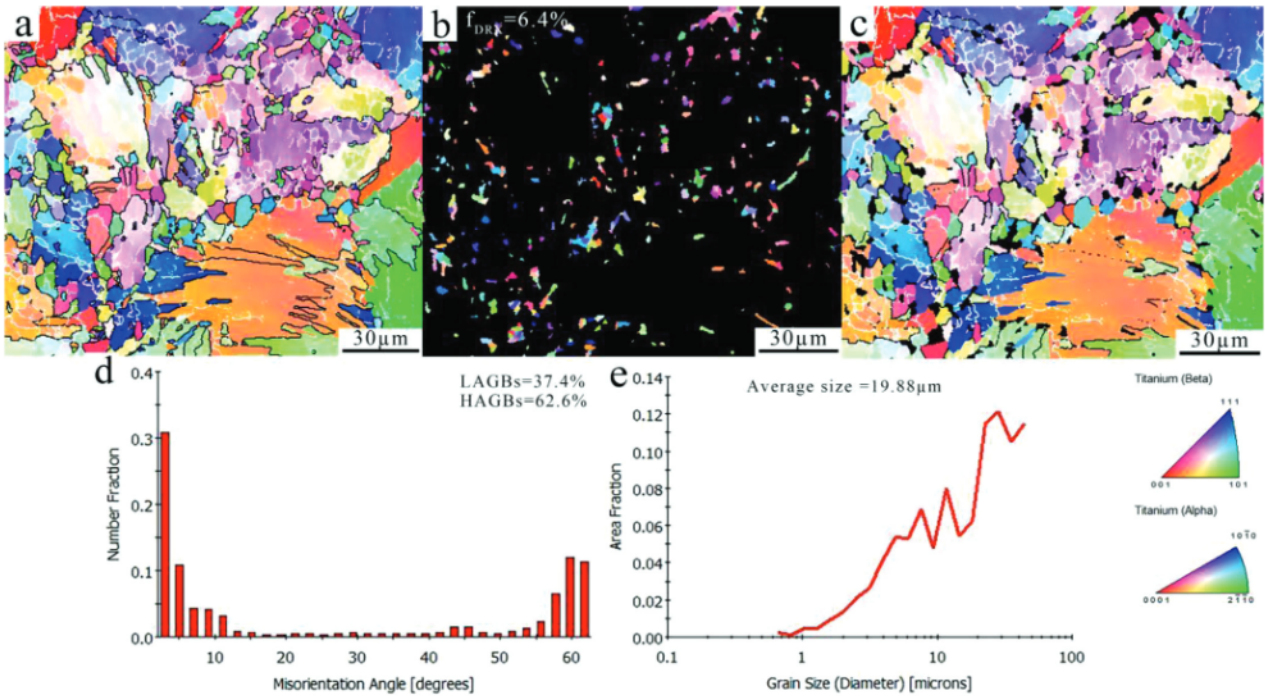

Figure 6: EBSD analysis results for one-pass deformation at 950 °C: a) IPF, b) DRXed grains, c) coarse grains, d) misorientation distribution, e) grain size

SEM image (**Figure 5b**) shows that the microstructure of the α phase with the needle or acicular morphology was arranged in a cross-parallel arrangement along different directions with a typical basketweave structure, which included β grains and formed mostly on the original β grain boundaries.[19] **Figure 6** shows an EBSD analysis of all grains: DRXed grains and coarse grains at 0.1 s^{-1} during one-pass deformation. The fraction of DRX (f_{DRX}) for one-pass deformation was 6.4 % (**Figure 6b**). Additionally, the average grain size, the fraction of high-angle grain boundaries (HAGBs) and low-angle grain boundaries (LAGBs) were 19.88 μm, 62.6 % and 37.4 %, respectively, as shown in **Figures 6d** and **6e**. It can also be seen from **Figure 6c** that dynamic recrystallization mainly occurred at the intersection and kink regions of grain boundaries, which was also found in high-tensile Ti-6Al-4V alloy with initial coarse equiaxed phases.[3]

3.2.2. Microstructure of the HIPed Ti-6Al-4V alloy after two-pass deformation

Figure 7 shows the microstructure of the HIPed Ti-6Al-4V alloy after two-pass deformation at the deformation temperature of 900 °C and different strain rates. As it can be seen in **Figures 7a** and **7d**, the coarse equiaxed β grains formed during one-pass deformation further grew at the strain rate of 1 s^{-1} during two-pass deformation; there are a large amount of an acicular martensite structure and a small amount of a lath martensite structure in the β grains. This is mainly due to the long time and high deformation temperature during rapid quenching, promoting a continuous growth of β grains and the precipitation of martensite. It can be seen on **Figures 7a**, **7b** and **7c** that with the increase in the strain rate, the content of the equiaxed α phase was increased and distorted β grain boundaries mainly occurred, which was mainly due to a kinked grain-boundary intersection and grain-boundary separation spheroidisation during two-pass deformation. This is mainly the result of the formation of sub-grain boundaries inside the originally stable lamellar α phase and recrystallized grains inside the α phase, which was also found by Margolin[20] in the study on a titanium alloy with a widmanstatten structure. Due to the surface tension, the β phase easily entered the newly formed α/α interface (**Figure 7f**).

With the continuous penetration of the β phase, the α phase gradually separated to form new α grains. It can also be seen in **Figures 7b**, **7c** and **7d** that the α phase at the β grain boundary was distorted and broken, which occurred at the intersection of β grains and near the deformation zone. This was mainly due to the insufficient phase transition from the initial α phase to the β phase after two-pass deformation and the facts that some of the β phase and a small amount of the α phase were broken, forming finer grains. **Figures 7e** and **7f** show the spheroidisation of the initial lamellar α, which mainly occurred in the area of large deformation. The lamellar α phase was elongated, deflected and kinked at the same time during the large deformation along the compressing direction. Due to the atomic diffusion, the β phase gradually diffused into the sub-structure of the lamellar α phase and some lamellar α phase was gradually segregated along the sub-structure, or was directly segregated due to the localized shearing with further deformation, as shown in **Figure 7f**.

Weiss and Peter[21,22] found that the mechanisms for the separation of lamellar α into shorter segments are the

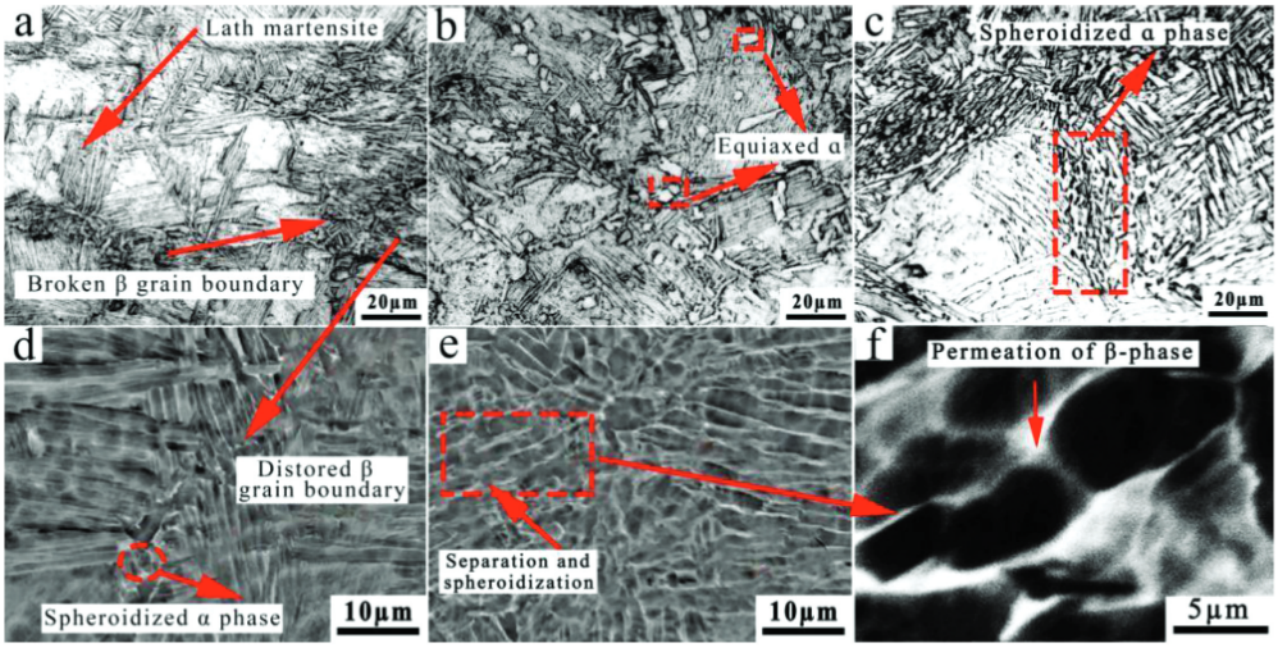

Figure 7: OM and SEM images of HIPed Ti-6Al-4V alloy after two-pass deformation at the temperature of 900 °C and different strain rates: a) and d) 1 s^{-1}, b), e) and f) 0.1 s^{-1}, c) 0.01 s^{-1}

formation of sub-boundaries across the α plate, and the localized shear and rotation of lamellar α during hot deformation. The driving force of spheroidisation is a decrease in the surface energy, which promotes the penetration of the β phase into the α phase.[23] **Figure 8** shows the EBSD analysis of all grains, DRXed grains and coarse grains at 0.1 s^{-1} during two-pass deformation. The fraction of DRX (f_{DRX}) for two-pass deformation was 10 % (**Figure 8b**). Additionally, the average grain size and the fraction of high-angle grain boundaries (HAGBs) and low-angle grain boundaries (LAGBs) were 10.56 μm, 80 % and 20 %, respectively, as shown in **Figures 8d** and **8e**. This was different from one-pass deformation as a large number of substructures appeared in the lamellar α phase, gradually separated and spheroidized with the permeation of the β phase during two-pass deformation. So, a large number of bent lamellar and equiaxed α-phase mixed structures were observed in **Figure 8a**.

3.2.3. Microstructure of the HIPed Ti-6Al-4V alloy after three-pass deformation

Figure 9 shows the microstructure of the HIPed Ti-6Al-4V alloy after three-pass deformation at 850 °C with different strain rates. As seen in **Figure 9b**, the martensitic structure was transformed into a mixture of α and β phases consisting of the β-transformed phase, in which the α phase was present as a fine needle-like structure. The microstructures of the specimens obtained after the three-pass deformation at 0.1 s^{-1} exhibit a tri-modal structure, which include the equiaxed α phase, lamellar α phase and β-transformed phase (β_t). The volume fraction and size of the equiaxed α phase, the width of the lamellar α phase and the volume fraction of the β-transformed phase (β_t) characterize the morphology of the microstructure of the HIPed Ti-6Al-4V alloy after three-pass deformation at different strain rates, measured and shown in **Table 4**. From **Table 4**, it can be seen that the volume fraction of the equiaxed α phase increased with a decrease in the strain rate at the deformation temperature of 850 °C, while the size of the equiaxed α phase had a different trend. In addition, the size of the equiaxed α phase and the width of lamellar α decreased from 3.46 μm to 2.44 μm and from 2.16 μm to 1.68 μm as the strain rate decreased, respectively. The main reason for this is the fact that with the decrease in the variable rate, the lamellar α phase has more time for spheroidisation and, at the same time, more recrystallized grains appear due to the strain accumulation, so the grain size decreases.[24]

Compared with two-pass deformation, the fraction of the equiaxed α phase increased and its size decreased, indicating that dynamic recrystallization occurred during three-pass deformation, which is also confirmed with the dynamic-recrystallization-grain map from **Figure 10b**. As shown in **Figures 9d, 9e** and **9f**, the spheroidisation of lamellar α was mainly due to the deformation leading to the formation of sub-grain boundaries inside the originally stable lamellar α phase, which caused the β phase to permeate into the lamellar α phase, forming a new α/β interface, and the lamellar structure to be transformed into a spherical structure.[25] Therefore, after three-pass deformation, the spheroidisation of lamellar α mainly occurred due to grain boundary separation spheroidisation. It can also be seen that the content of the equiaxed α phase increased gradually with the decrease

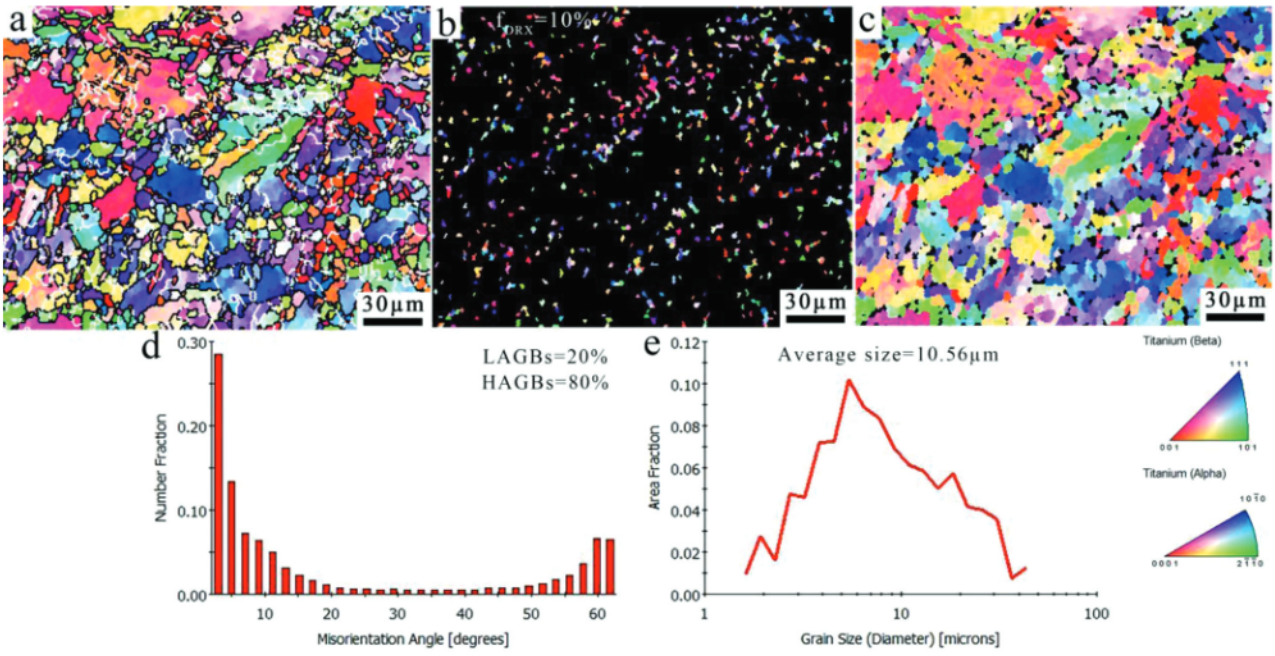

Figure 8: EBSD analysis results for two-pass deformation at 900 °C: a) IPF, b) DRXed grains, c) coarse grains, d) misorientation distribution, e) grain size

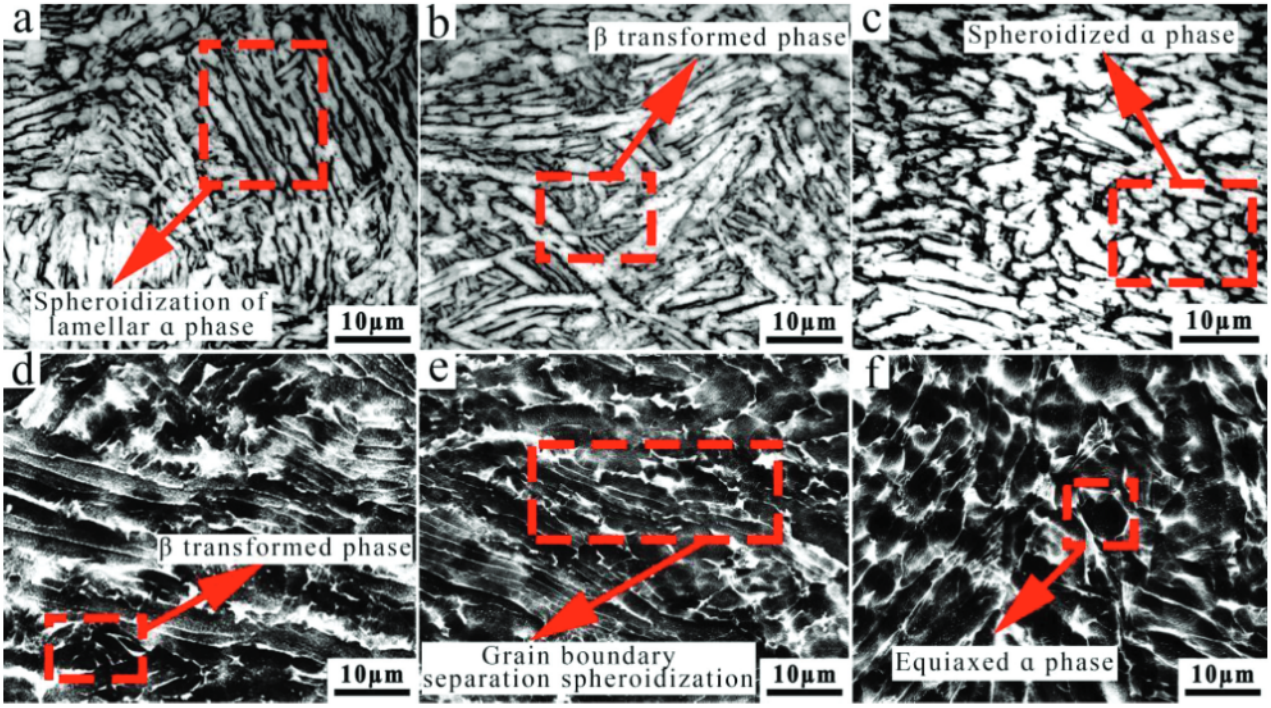

Figure 9: OM and SEM images of HIPed Ti-6Al-4V alloy after three-pass deformation at the temperature of 850 °C and different strain rates: a) and d) 1 s^{-1}, b) and e) 0.1 s^{-1}, c) and f) 0.01 s^{-1}

in the strain rate, which was mainly due to enough time for the nucleation and growth at a low strain rate.[26]

Compared with the two-pass deformation specimens, the microstructure of the compressed specimen lost the α phase at the prior β grain boundary and transformed into an equiaxed and lamellar α phase, mainly contributing to the distortion and fracturing of the α phase of the prior β grain boundary during long-term deformation. In this experiment, under certain temperature and deformation conditions, the thickness of lamellar α gradually decreased, but the content of the β-transformed phase gradually increased with the decrease in the strain rate, indicating that the secondary lamellar α phase precipitated into the prior β phase during three-pass deformation. Semiatin and Bieler[27] studied the effect of α platelet thickness on the plastic flow of Ti–6Al–4V with a β-transformed microstructure, showing that the thickness of the lamellar α phase was noticeably influenced by the deformation parameters and initial microstructure.

It can be seen from **Figure 9c** that the microstructure of the tested specimens consists of the equiaxed and lamellar α phase + β-transformed phase (β_t) whose microstructure proportions were 11.4 %, 65.1 % and 23.5 % at the strain rate of 0.1 s^{-1}, respectively. With the decrease in the strain rate from 1 s^{-1} and 0.1 s^{-1} to 0.01 s^{-1}, the β-transformed phase (β_t) correspondingly increased from 20.1 % and 23.5 % to 26.7 %, as shown in **Table 4**. It can be concluded that the strain rate mainly affects the content of the β-transformed phase and the spheroidisation of the lamellar α phase during three-pass deformation. The mechanism of the microstructure evolution during three-pass deformation was different from that during two-pass deformation. The differences are in the volume fraction of the equiaxed α phase, and the spheroidisation mechanism of the second lamellar α phase and β-transformed structure.

Figure 10 shows the EBSD analysis of all grains, DRXed grains and coarse grains at 0.1 s^{-1} during three-pass deformation. The fraction of DRX (f_{DRX}) for three-pass deformation was 47 % (**Figure 10b**). Additionally, the average grain size, the fraction of high-angle grain boundaries (HAGBs) and low-angle grain boundaries (LAGBs) were 4.56 μm, 41 % and 59 %, respectively, as shown in **Figures 10d** and **10e**. Compared with one-pass and two-pass deformation, the fraction of DRX (f_{DRX}) increased from 6.4 % and 10 % to 47 % during three-pass deformation and the increased extent of DRX (f_{DRX}) was 40.6 % and 37 %, respectively (**Figure 10b**). It can be found that the proportion of low-angle grain boundaries (LAGBs) was the largest compared with the one-pass and two-pass deformation. The appearance of low-angle grain boundaries (LAGBs) indicated that the initial lamellar α phase was divided into many fine equiaxed subgrains by sub-boundaries, and spheroidisation occurred during recrystallization, indicating that the formation of sub-grains or sub-grain boundaries is a necessary stage for the spheroidisation of a lamellar α phase.

Lin et al.[3] found that the dynamic-softening behavior is mainly induced by a severe dynamic globularization of lamellar α phases, accompanied by the formation of HAGBs of a Ti-6Al-4V alloy with thick lamellar micro-

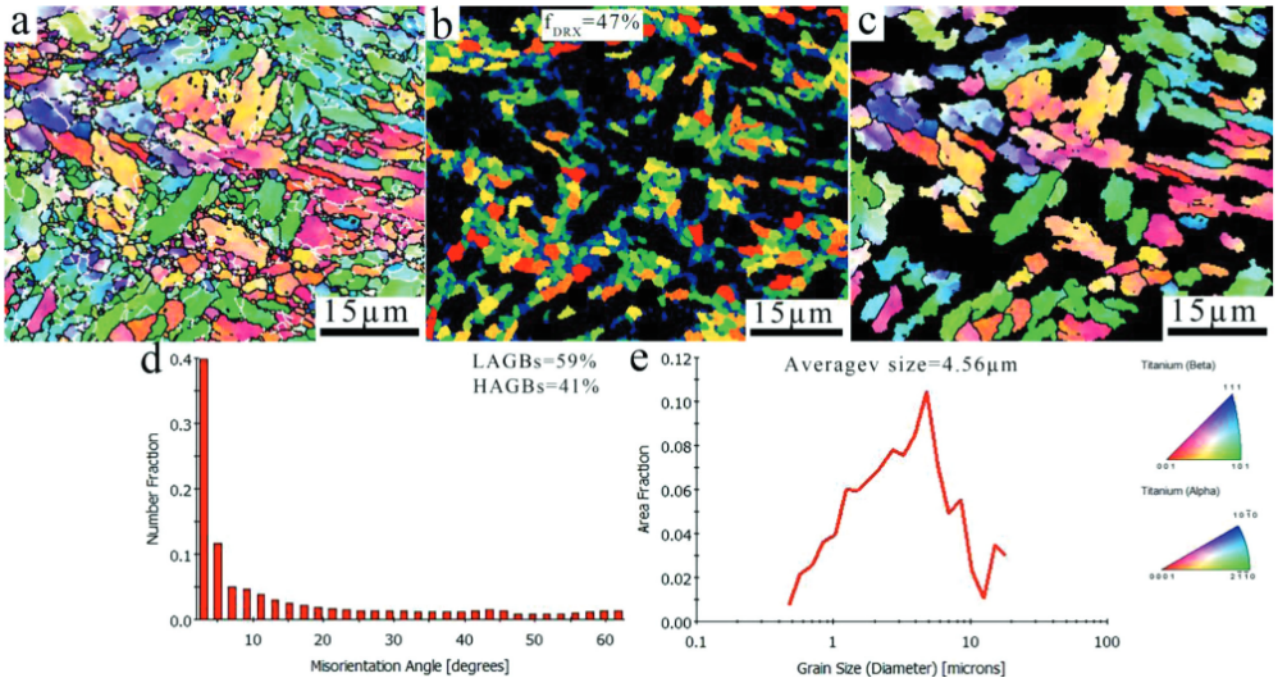

Figure 10: EBSD analysis results for three-pass deformation at 850 °C: a) IPF, b) DRXed grains, c) coarse grains, d) misorientation distribution, e) grain size

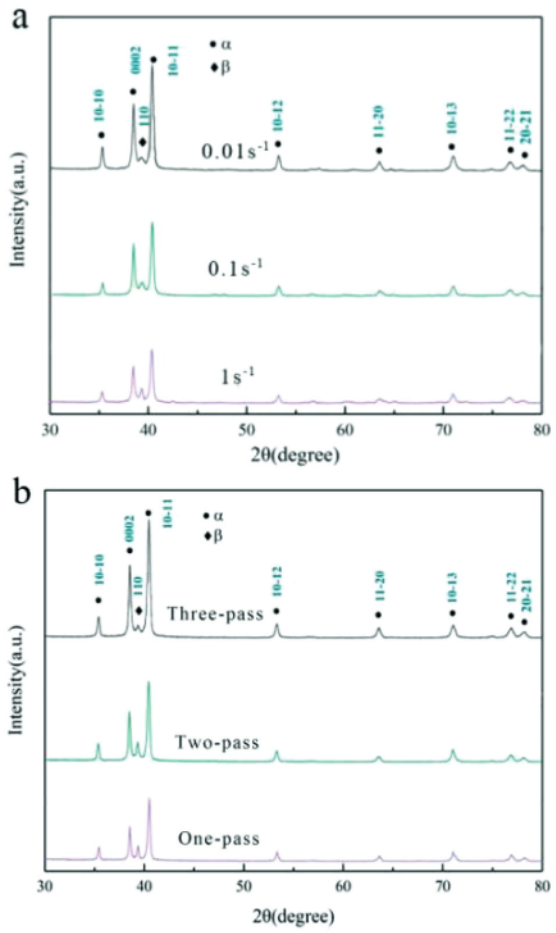

Figure 11: XRD patterns of HIPed Ti-6Al-4V alloy for: a) three-pass deformation at different strain rates, b) different deformation passes at 0.1 s^{-1}

structures during uniaxial hot tensile deformation. It can be concluded that recrystallization is beneficial for the spheroidisation of the lamellar α phase. **Figure 11** shows X-ray diffraction (XRD) patterns at different conditions. It can be observed that the diffraction peak of the α lattice plane of (0002) and (10-11) increased with the increase in the strain rate and deformation passes, as shown in **Figures 11a** and **11b**. The (110) β peak at 39.5° changed little with respected to the strain rate, but it increased with the increased deformation passes (**Figure 11**). It can be concluded that the strain rate has little effect on the content of the β phase, which gradually decreases with the increase in the deformation passes; this is mainly due to the deformation temperature that gradually becomes lower than the β-phase transition point. This phenomenon was also found by Ji when investigating the flow softening and dynamic transformation of a Ti-6Al-4V alloy in the two-phase region during hot deformation.[28]

Table 4: Microstructure parameters of HIPed Ti-6Al-4V alloy after three-pass deformation

Strain rate (s^{-1})	Volume fraction of equiaxed α phase (%)	Size of equiaxed α (μm)	Width of lamellar α (μm)	Volume fraction of β_t (%)
1	8.2	3.46	2.16	20.1
0.1	11.4	3.28	1.79	23.5
0.01	15.1	2.44	1.68	26.7

3.3. Microhardness of the HIPed Ti-6Al-4V alloy

Figure 12 shows the microhardness of the specimens of the HIPed Ti-6Al-4V alloy after multi-pass and single-pass deformation at different deformation parameters. The microhardness of titanium alloy is affected by many factors such as deformation temperature, strain rate, deformation amount, phase content and distribution, and microstructure morphology. **Figure 12a** shows that the microhardness of the tested specimens decreases with the increase in the deformation temperature at the strain rate of 1 s^{-1}. It can be concluded that the microhardness changes from 351.5 HV and 330.1 HV to 315.4 HV with the increase in the temperature under constant deformation and strain rate, indicating that the temperature has a great influence on it. According to the analysis from **Figure 4** and **Table 3**, where the strain rate and strain were constant, the volume and size of the α phase increased with the decrease in the temperature during single-pass deformation. The results show that the Ti-6Al-4V alloy is an $\alpha + \beta$ alloy, in which the α and β phase are body-centered cubic (BCC) and hexagonal close-packed (HCP) structures, respectively. So, during single-pass deformation, the increase in the microhardness with the increase in the temperature is mainly caused by the content of the α phase.

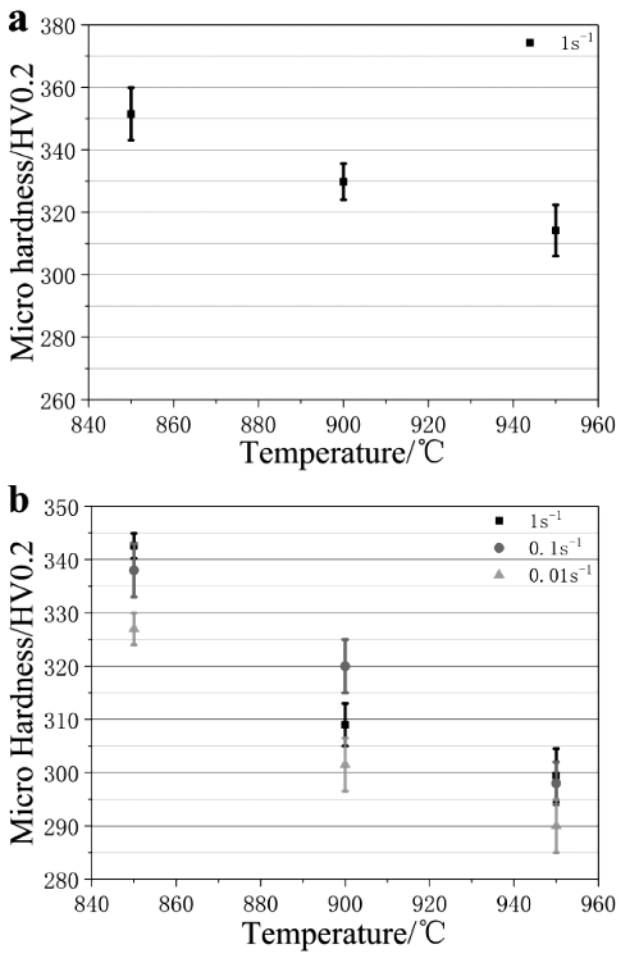

Figure 12: Microhardness of HIPed Ti-6Al-4V alloy: a) single-pass deformation, b) multi-pass deformation

Figure 12b shows the microhardness of the tested specimens after multi-pass deformation at different strain rates. The result shows that the microhardness increased with the increase in the deformation passes. When the strain rate was 1 s^{-1}, the microhardness of the tested specimen increased from 299.5 HV and 309.1 HV to 342.6 HV with the increase in the deformation passes. It also can be found that the microhardness increased with the increase in the strain rate under a certain amount of deformation. During multi-pass deformation, with the increase in the deformation passes, the microhardness of the tested sample also gradually increased with the increase in deformation from 20 % and 40 % to 70 %, as shown in **Figure 12b**. This is mainly due to the fact that the increase in the strain and decrease in the deformation temperature from 950 °C and 900 °C to 850 °C with the increase in the deformation passes, resulted in a gradually increased content of the α phase, ascribed to the strain-enhanced β/α phase transformation, causing an increase in the microhardness.

He and Dehghan[29] studied the microstructure development during the concurrent hot deformation and β/α phase transformation in a Ti-6Al-4V alloy, and found that an improvement in the grain refinement and phase transformation was ascribed to the strain-enhanced β/α phase transformation. When the deformation passes of multi-pass deformation are defined, the microhardness values show an increasing trend with the increase in the strain rate; the microhardness values at strain rates ranging from 0.01 s^{-1} and 0.1 s^{-1} to 1 s^{-1} during three-pass deformation are 342.6 HV, 338.1 HV and 327.2 HV, respectively. According to the analysis from **Figure 9** and **Table 4**, the volume of the equiaxed α phase decreased with the increase in the strain rate; however, its size and the width of the lamellar α phase increased with the increase in the strain rate, which shows that the α phase has a great influence on the microhardness. Compared with the single-pass deformation analysis, it can be seen that the microhardness of the Ti-6Al-4V alloy is greatly affected by the content, size and morphology of the α phase.

4 CONCLUSION

Multi-pass and single-pass deformations were carried out to investigate their effects on the hot-deformation behavior, microstructural evolution and microhardness of a HIPed Ti-6Al-4V alloy. The microstructure was characterized with an optical microscope and scanning electron microscope (SEM). The microhardness of the tested specimens were measured via the Vickers hardness test at room temperature. The following conclusions are attained from the experiment results:

1) During single-pass and multi-pass deformations, all the true stress-strain curves exhibited a peak stress,

followed by different flow-softening extents. The softening extent of single-pass deformation was obvious at a low temperature and strain rate, and recrystallization was the main softening mode. However, with respect to multi-pass deformation, the softening extent of three-pass deformation was more obvious than those of one-pass and two-pass deformation. Based on the observation of the microstructures, one-pass and two-pass deformations mainly led to a distortion and spheroidisation of the lamellar α phase and fractures of grain boundaries, while dynamic recrystallization mainly occurred during three-pass deformation, which is the main softening mechanism of this process.

2) After the multi-pass deformation at the temperature range from 950 °C and 900 °C to 850 °C, the primary β grains were elongated along the flow direction and some of β grains began to blend. As α boundaries began to fracture during one-pass deformation, there were a lot of distorted and broken grain boundaries due to the spheroidisation after two-pass deformation and, finally, spheroidisation and dynamic recrystallization occurred and the spheroidisation ratio increased with the increase in the strain rate, while the volume fraction of β_t also increased, exhibiting a tri-modal microstructure including the equiaxed α phase, lamellar α phase and β-transformed phase (β_t) at 0.1 s^{-1} after three-pass deformation.

3) The microhardness of the HIPed Ti-6Al-4V alloy during multi-pass deformation increased with the increase in deformation passes. When the strain rate was 1 s^{-1}, the microhardness of the tested specimen increased from 299.5 HV and 309.1 HV to 342.6 HV with the increase in deformation passes. It can also be seen that the microhardness increased with the increase in the strain rate under a certain amount of deformation.

Acknowledgments

The present research was supported by the National Natural Science Foundation of China (Grant No. 51675492).

Conflicts of Interest

We declare that we have no financial or personal relationships with the other people or organizations that could inappropriately influence our work; there is no professional or other personal interest of any nature or kind in any product service and/or company that could be seen as influencing the position presented in this article, or a review of it.

5 REFERENCES

[1] Y. Sun, G. Q. Luo, J. Zhang, C. D. Wu, J. Li, Q. Shen, Phase transition, microstructure and mechanical properties of TC4 titanium alloy prepared by plasma activated sintering, Journal of Alloy and Compounds, 741 (**2018**), 918–926, doi:10.1016/j.jallcom.2018.01.197

[2] L. C. Zhang, L. Y. Chen, A review on biomedical titanium alloys: recent progress and prospect, Advanced Engineering Materials, 21 (**2019**), 1–29, doi:10.1002/adem.201801215

[3] Y. Q. Jiang, Y. C. Lin, X. Y. Jiang, D. G. He, N. Kotkunde, Hot tensile properties, microstructure evolution and fracture mechanisms of Ti-6Al-4V alloy with initial coarse equiaxed phases, Materials Characterization, 163 (**2020**), 1–8, doi:10.1016/j.matchar.2020.110272

[4] Y. C. Lin, Y. Tang, X. Y. Zhang, C. Chen, H. Yang, K. C. Zhou, Effects of solution temperature and cooling rate on microstructure and micro-hardness of a hot com- pressed Ti-6Al-4V alloy, Vacuum, 159 (**2019**), 191–199, doi:10.1016/j.vacuum. 2018.10.035

[5] K. Wang, M. Q. Li, Q. Liu, Evolution mechanisms of the primary α and β phases during α/β deformation of an α/β titanium alloy TC8, Materials Characterization, 120 (**2016**), 115–123, doi:10.1016/j.matchar.2016.08.028

[6] Y. C. Lin, C. Y. Zhao, M. S. Chen, D. D. Chen, A novel constitutive model for hot deformation behaviors of Ti-6Al-4V alloy based on probabilistic method, Applied Physics A, 122 (**2016**), 716–720, doi:10.1007/s00339-016-0248-8

[7] L. Xu, R. P. Guo, C. G. Bai, J. F. Lei, R. Yang, Effect of hot isostatic pressing conditions and cooling rate on microstructure and properties of Ti-6Al-4V alloy from atomized powder, Journal of Materials Science and Technology, 30 (**2014**), 1289–1295, doi:10.1016/j.jmst.2014.04.011

[8] Y. Kim, Y. B. Song, S. H. Lee, Y. S. Kwon, Y. B. Song, Characterization of the hot deformation behavior and microstructural evolution of Ti-6Al-4V sintered preforms using materials modeling techniques, Journal of Alloys and Compounds, 676 (**2016**), 15–25, doi:10.1016/j.jallcom. 2016.03.146

[9] P. F. Gao, H. Yang, X. G. Fan, Z. N. Lei, Y. Cai, Prediction of tri-modal microstructure under complex thermomechanical processing history in isothermal local loading forming of titanium alloy, Transactions of Nonferrous Metals Society of China, 27 (**2017**), 2423–2433, doi:10.1016/S1003-6326(17)60269-3

[10] Z. X. Zhang, S. J. Qu, A. H. Feng, J. Shen, D. L. Chen, Hot deformation behavior of Ti-6Al-4V alloy: effect of initial microstructure, Journal of Alloys and Compounds, 718 (**2017**), 170–181, doi:10.1016/j.jallcom.2017.05.097

[11] Y. Kim, E. P. Kim, Y. B. Song, S. H. Lee, Y. S. Kwon, Microstructure and mechanical properties of isostatically pressed Ti-6Al-4V alloy, Journal of Alloys and Compounds, 603 (**2014**), 207–212, doi:10.1016/j.jallcom.2014.03.022

[12] M. Wang, J. X. Zhou, Y. J. Yin, H. Nan, P. J. Xue, Z. X. Tu, Hot deformation behavior of the Ti-6Al-4V alloy prepared by powder hot isostatic pressing, Journal of Alloys and Compounds, 721 (**2017**), 320–332, doi:10.1016/j.jallcom.2017.06.003

[13] Z. X. Zhang, S. J. Qu, A. H. Feng, X. Hu, J. Shen, Microstructural mechanisms during multidirectional isothermal forging of as-cast Ti-6Al-4V alloy with an initial lamellar microstructure, Journal of Alloys and Compounds, 773 (**2019**), 277–287, doi:10.1016/j.jallcom.2018.09.220

[14] Y. J. Wu, H. J. Liu, J. Xu, Z. Zhang. Y. Xue, Constitutive equations and processing map for hot deformation of a Ti-6Al-4V alloy prepared with spark-plasma sintering, Mater. Tehnol., 54 (**2020**), 25–32, doi:10.17222/mit.2019.087

[15] R. Liu, B. Wang, J. Li, W. Ma, Deformation behavior and microstructure evolution of powder metallurgy Ti-6Al-4V alloy during hot compression, Journal of Materials Engineering and Performance, 28 (**2019**), 4454–4466, doi:10.1007/s11665-019- 04166-0

[16] X. N. Peng, H. Z. Guo, T. Wang, Z. K. Yao, Effects of β treatments on microstructures and mechanical properties of TC4-DT titanium alloy, Materials Science and Engineering A, 553 (**2012**), 55–63, doi:10.1016/j.msea.2011.11.033

[17] Y. C. Lin, X. Y. Jiang, C. J. Shuai, C. Y. Zhao, D. G. He, M. S. Chen, C. Chen, Effects of initial microstructures on hot tensile deformation behaviors and fracture characteristics of Ti-6Al-4V alloy, Materials Science and Engineering A, 711 (**2018**), 293–302, doi:10.1016/j.msea.2017.11.044

[18] X. Tan, Y. Kok, J. T. Yu, G. Vastola, An experimental and simulation study on build thickness dependent microstructure for electron beam melted Ti-6Al-4V, Journal of Alloys and Compounds, 646 (**2015**), 303–309, doi:10.1016/j.jallcom.2015.05.178

[19] S. Roy, S. Suwas, The influence of temperature and strain rate on the deformation response and microstructural evolution during hot compression of a titanium alloy Ti-6Al-4V-0.1B, Journal of Alloys and Compounds, 548 (**2013**), 110–125, doi:10.1016/j.jallcom.2012.08.123

[20] N. Stefansson, S. L. Semiatin, D. Eylon, The kinetics of static globularization of Ti-6Al-4V, Metallurgical & Materials Transactions A, 33 (**2002**), 3527–3534, doi:10.1007/s11661-002-0340-x

[21] I. Weiss, F.H. Froes, D. Eylon, G.E. Welsch, Modification of alpha morphology in Ti-6Al-4V by thermomechanical processing, Metallurgical Transactions A, 17 (**1986**), 1935–1947, doi:10.1007/BF02644991

[22] M. Peter, G. Luetjering, G. Eylon, Control of microstructures of (alpha + beta) titanium alloys, Zeitschrift Metallkunde, 74 (**1983**), 274–282

[23] R. Ding, Z. X. Guo, A. Wilson, Microstructural evolution of a Ti–6Al–4V alloy during thermomechanical processing, Materials Science and Engineering A, 327 (**2002**), 233–245, doi:10.1016/S0921-5093(01)01531-3

[24] S. Cao, Q. Hu, A. Huang, Z. Chen, M. Sun, J. Zhang, C. Fu, Q. Jia, C. V. S. Lim, R. R. Boyer, Static coarsening behaviour of lamellar microstructure in selective laser melted Ti-6Al-4V, Journal of Materials Science and Technology, 35 (**2019**), 1578–1586, doi:10.1016/j.jmst.2019.04.008

[25] T. Seshacharyulu, S. C. Medeiros, J. T. Morgan, J. C. Malas, W. G. Frazier, Y. V. R. K. Prasad, Hot deformation mechanisms in ELI grade Ti-6A1-4V, Scripta Materialia, 41 (**1999**), 283–288, doi:10.1016/s1359-6462(99)00163-3

[26] G. A. Sargent, A. P. Zane, P. N. Fagin, A. K. Ghosh, S. L. Semiatin, Low-temperature coarsening and plastic flow behavior of an alpha/beta titanium billet material with an ultrafine microstructure, Metallurgical and Materials Transactions A, 39 (**2008**), 2949–2964, doi:10.1007/s11661-008-9650-y

[27] S. L. Semiatin, T. R. Bieler, The effect of alpha platelet thickness on plastic flow during hot working of Ti-6Al-4V with a transformed microstructure, Acta Materialia, 49 (**2001**), 3565–3573, doi:10.1016/S1359-6454(01)00236-1

[28] X. Ji, H. Yu, B. Guo, F. Jiang, J. J. Jonas, Post-dynamic α to β phase transformation and reverse transformation of Ti-5Al-3V alloy after hot deformation in two phase region, Materials and Design, 188 (**2020**), 1–10, doi:10.1016/j.matdes.2019.108466

[29] L. J. He, A. Dehghan-Manshadi, R. J. Dippenaar, The evolution of microstructure of Ti-6A1-4V alloy during concurrent hot deformation and phase transformation, Materials Science and Engineering A, 549 (**2012**), 163–167, doi:10.1016/ j.msea.2012.04.025